Int. J. Electrochem. Sci., 17 **(2022)** Article Number: 221023, doi: 10.20964/2022.10.21

International Journal of
ELECTROCHEMICAL
SCIENCE
www.electrochemsci.org

An electrochemical biosensor based on hemoglobin and FeS@MoS_2-C nanocomposite for nitrite, hydrogen peroxide and bromate detection

Siyue Zhang[1], Hui Cheng[1], Baoli Wang[1], Fan Shi[1], Lijun Yan[1], Lina Zeng[2,], Lin Li[2], Shuhai He[3], Wei Sun[1*]*

[1] Key Laboratory of Laser Technology and Optoelectronic Functional Materials of Hainan Province, Key Laboratory of Functional Materials and Photoelectrochemistry of Haikou, College of Chemistry and Chemical Engineering, Hainan Normal University, Haikou 571158, China
[2] College of Physics and Electronic Engineering, Hainan Normal University, Haikou 571158, China
[3] Hainan Ecological Environmental Monitoring Center, 98 Baiju Avenue, Haikou 571126, China
[*]E-mail: zenglinahainan@126.com, sunwei@hainnu.edu.cn

Received: 28 June 2022 / *Accepted:* 4 August 2022 / *Published:* 10 September 2022

Petal-shaped FeS@MoS_2-C nanocomposite was synthesized using carbon fiber as the basic carrier by hydrothermal method. The uniformly dispersed nanocomposite, hemoglobin (Hb) and Nafion mixture were drip-coated on the newly prepared carbon ionic liquid electrode (CILE) to build a modified electrode named as Nafion/Hb/FeS@MoS_2-C/CILE. The morphology and valence state of FeS@MoS_2-C nanocomposite was investigated by SEM, TEM, XPS etc. and the biological structure of Hb was not changed based on UV-VIS and FT-IR spectroscopic analysis. Electrochemistry of Nafion/Hb/FeS@MoS_2-C/CILE was recorded by cyclic voltammetry with voltammetric behaviors investigated. Also, the modified electrode has excellent catalytic performance for nitrite, hydrogen peroxide, bromate with the detection range as 0.10~5.00 mmol L^{-1}, 0.10~14.00 mmol L^{-1}, 0.05~25.00 mmol L^{-1}, respectively. The pickle juice sample was analyzed by this method satisfactory, further proving the practical application.

Keywords: FeS@MoS_2-C nanocomposite, hemoglobin, electrochemistry, electrocatalysis

1. INTRODUCTION

Electrochemical sensors have emerged as novel diagnostic tools that integrates electrochemical analysis with sensing technology [1, 2], which are becoming increasingly significant in daily life owns of their advantages such as rapidity, easy miniaturization, portability, possibility of on-site analysis and low cost [3, 4]. Hemoglobin (Hb) is a commonly used peroxidase-like protein, and the bound prosthetic groups in Hb (heme or iron groups) play key role in the O_2 binding and transporting in the human body

with reversible way [5]. Also Hb-based electrochemical sensors are depended on direct electron transfer (DET) of Fe(III)/Fe(II) couple, which can explore the pathologies associated with aberrant heme degradation and develop emerging medical countermeasures [6]. However, the realization of the DET process of Hb molecules on the traditional solid electrodes is difficult with slow electron transfer rate, which is due to the deeply surround of Hb inside the hydrophobic structure [7]. Therefore, nanomaterials modified electrode is an efficient way to realize DET process between electrode and Hb. Various nanomaterials and composites such as porous biomass carbon biochar, Au nanoparticles, black phosphorene, carbon nanofiber, graphene etc. have been used for the construction of Hb-based electrochemical sensors, which exhibit good electrochemical performances and electrocatalysis behaviors [8-15].

Notably, reasonably and intelligently synthesis of nanomaterials for electrode modification may lead to the improvement of performance of the electrochemical sensor. Recently molybdenum disulfide (MoS_2) and related composites has attracted considerable interests due to its unique merits including good conductivity, chemical stability and especially low cost [16]. For example, Yang et al used a hydrothermal method to synthesize 3D molybdenum disulfide/reduced graphene oxide composites for H_2O_2 detection with linear range from 2.0 μmol L^{-1} to 23.18 mmol L^{-1} and the detection limit of 0.19 μmol L^{-1} [17]. Liu et al prepared efficient g-C_3N_4-MoS_2 hybrids nanocomposite for detecting sulfide ions with the detection limit as low as 37 nM [18]. Chen et al successfully constructed MoS_2-AuPt nanocomposite modified electrode for quantitative detection of lactic acid with the detection limit of 0.00033 mM, response time smaller than 15 s, good sensitivity and wide linear range [19].

Inspired by these pioneering works above, FeS@MoS_2-C was fabricated by a simple one-step hydrothermal process and further employed to construct a Nafion/Hb/FeS@MoS_2-C/CILE as the electrochemical sensor. Various characterization methods such as X-ray photoelectron spectroscopy (XPS), scanning electron microscopy (SEM), transmission electron microscopy (TEM), UV-vis and FT-IR spectroscopy were performed to record the morphology and structure of the material used. Cyclic voltammetry (CV) was employed to study the electrochemical processes and electrocatalysis. Benefit from the flower-like structure that can greatly enlarge the effective surface area of the electrode and provide more active sites for the electrocatalysis, this electrochemical sensor exhibits good analytical performances with high stability and repeatability.

2. EXPERIMENTAL SECTION

2.1 Apparatus

CHI 660E electrochemical workstation (Shanghai CH Instruments, China) with three-electrode system: Nafion/Hb/FeS@MoS_2-C/CILE (Φ = 4.0 mm) as working electrode, Ag/AgCl as reference electrode and platinum electrode as auxiliary electrode., UV-Visible spectrophotometer (Mettler-Toledo, USA), Nicolet 6700 FT-IR spectrophotometer (Thermo Fisher Scientific, USA), JEM 2010F transmission electron microscopy (TEM, JEOL, Japan), JSM-7100F scanning electron microscopy

(SEM, JEOL, Japan), AXIS HIS 165 X-ray electron spectroscopy (XPS, Kratos Analytical, UK),

2.2 Reagents

Ferric nitrate nonahydrate ($Fe(NO_3)_3 \cdot 9H_2O$), sodium molybdate dihydrate ($Na_2MoO_4 \cdot 2H_2O$), thiourea (CH_4N_2S), potassium bromate and sodium nitrite (Shanghai Aladdin Reagent Co., Ltd., China), carbon fiber cloth (CFC, Hongkong Physichem. Co., Ltd., China), N-hexylpyridine hexafluorophosphate ($HPPF_6$, Lanzhou Yulu Fine Chem. Co., Ltd., China), 30%H_2O_2 (Sinopharm Group Co., Ltd., China).

2.3 Synthesis of FeS@MoS_2-C

Based on the reference [20], FeS@MoS_2-C was synthesized with the following procedure. 0.8 mmol Na_2MoO_4-$2H_2O$, 0.2 mmol $Fe(NO_3)_3 \cdot 9H_2O$, 1.0 mmol CH_4N_2S was stirred in 40 ml water for 20 min and dissolved without solid particles. Then the solution was transferred to a 50 ml Teflon autoclave together with CFC and kept at 200 °C for 24 h. After the reaction, the product was cooled naturally and washed with water.

2.4 Preparation of Nafion/Hb/FeS@MoS_2-C/CILE

CILE was home-made according to the reference [21]. Then 8.0 μL 2.0 mg/mL FeS@MoS_2-C suspension was dropped on the CILE surface. After drying at room temperature, 8.0 μL 15.0 mg/ml Hb solution and 0.5% Nafion solution were drip-coated step-by-step to successfully prepare Nafion/Hb/FeS@MoS_2-C/CILE.

3. RESULTS AND DISCUSSION

3.1 Morphological and structural characterizations

SEM images of FeS@MoS_2-C at different magnifications were shown as a homogeneous, micron petal-like structure with FeS nanoparticles overlaided on the petal sheet (Figure 1A-B). The spherical petal morphology greatly increases the effective surface area of the material and the FeS nanoparticles provide a great enhancement to the rapid transfer of electrons. The lamellar stripes of the petal structure can be seen by TEM (Figure 1C-D).

XPS was carried out to find the elemental composition of FeS@MoS_2-C as well as the chemical valence. The full XPS spectrum (Figure 2 A) shows that the elemental composition of the material includes C, O, N, S, Mo and Fe. The binding energies at 162.58 eV, 163.88 eV and 165.28 eV in the high-resolution XPS spectra of S 2p (Figure 2 B) correspond to Fe-S and Mo-S [22], respectively.

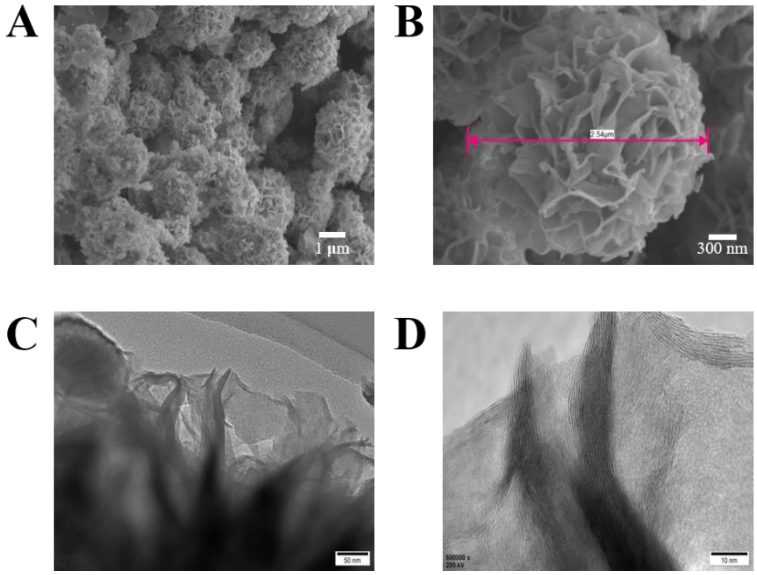

Figure 1. SEM images (A, B) and TEM images (C, D) of FeS@MoS_2-C

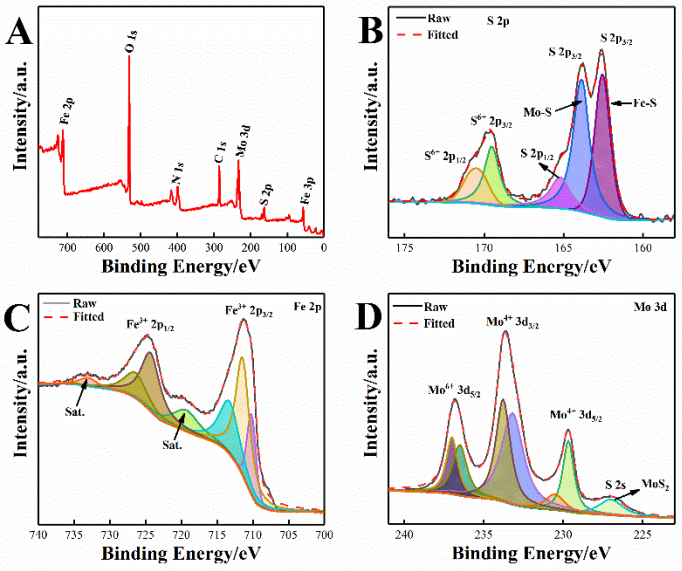

Figure 2. FeS@MoS_2-C of (A) XPS full spectrum; (B) S 2p; (C) Fe 2p; (D) Mo 3d

The XPS spectra of Fe 2p (Figure 2 C) exhibits the peaks at 710.18 eV, 711.58 eV and 713.58 eV that can be ascribed to the three binding energies of Fe^{3+} $2p_{3/2}$, and two peaks at 724.48 eV and 726.78 eV correspond to Fe^{3+} $2p_{1/2}$. Based on the binding energies of the two satellite peaks at 719.78 eV and 733.08 eV, the valence state of Fe in Fe 2p can be determined to be Fe^{3+} [23]. The XPS spectrum of Mo 3d (Figure 2 D) shows the binding energy of S 2s at 227.08 eV, corresponding to the compound MoS_2. Mo is present mainly as Mo^{4+} and Mo^{6+}, corresponding to the binding energies of 229.68 eV, 230.58 eV, 233.18 eV 233.78 eV, 236.48 eV, 236.98 eV.

3.2 Spectroscopic results

To illustrate the interaction of the FeS@MoS_2-C with Hb, UV-Vis absorption and FT-IR spectra were recorded and shown in Figure 3. In Figure 3 A, UV-Vis absorption spectrum proved that the absorption band of Hb appeared at 406.4 nm without change, indicating that the internal biostructure of Hb had not changed [24]. In Figure 3 B, FT-IR results showed that the characteristic peaks of Hb at 1538.99 cm^{-1} and 1650.85 cm^{-1}, also indicated that FeS@MoS_2-C did not destroy the biological structure of Hb [25].

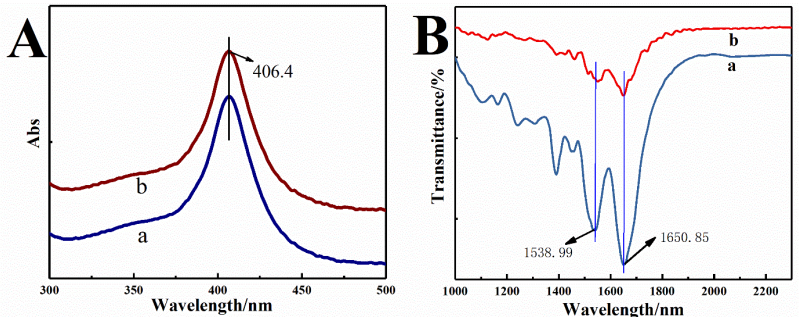

Figure 3. (A) UV-Vis absorption spectrum of (a) Hb; (b) Hb/FeS@MoS_2-C mixtrue; (B) FT-IR spectra of (a) Hb/FeS@MoS_2-C; (b) Hb

3.3 Electrochemical performances of the modified electrode

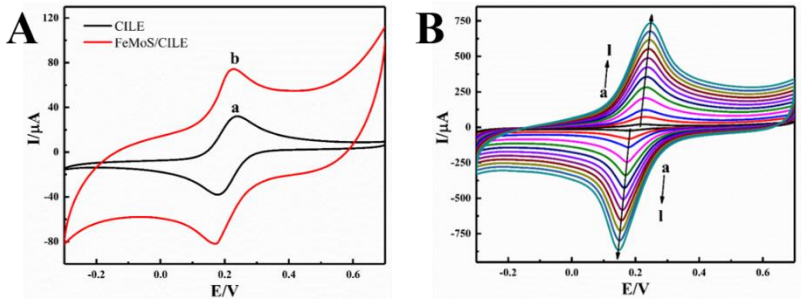

Figure 4. Cyclic voltammograms of (A) CILE (a), FeS@MoS_2-C/CILE (b) at scan rate of 0.10 V s^{-1}; (B) FeS@MoS_2-C/CILE with different scan rate (a-l: 0.01, 0.05, 0.10, 0.20, 0.30, 0.40, 0.50, 0.60, 0.70, 0.80, 0.90, 1.00 V s^{-1}) in 1.0 mmol L^{-1} K_3 [$Fe(CN)_6$] and 0.5 mol L^{-1} KCl solution.

To verify the voltammetric properties of the synthesized FeS@MoS_2-C, electrochemical behavior of FeS@MoS_2-C/CILE was investigated by measuring CV in a 1.0 mmol L^{-1} K_3 [$Fe(CN)_6$] and 0.5 mol L^{-1} KCl mixture. As shown in Figure 4A, the redox peak current of FeS@MoS_2-C/CILE (curve a) was obviously enhanced than that of CILE (curve a) with 2 times increment of peak currents, proving the presence of FeS@MoS_2-C accelerated the electron transfer. In addition, CV of FeS@MoS_2-C/CILE was further explored at different scan rates in the range from 0.01 to 1.0 V s^{-1} (Figure 4B). It could be seen that the redox peak current increased upon increasing of scan rate with the linear regression

equations as I_{pc} (μA) = 945.62 $\upsilon^{1/2}$ - 230.68 (n = 16, γ = 0.998) and I_{pa} (μA) = -682.22 $\upsilon^{1/2}$ + 160.79 (n = 16, γ = 0.997). Based on Randles-Sevcik formula [26], the effective surface area of FeS@MoS_2-C/CILE was 0.920 cm^2, showing that the petal-like structure of FeS@MoS_2-C on the electrode gave higher specific surface area.

3.4 Voltammetric behaviors of Nafion/Hb/FeS@MoS_2-C/CILE

CV of Nafion/Hb/FeS@MoS_2-C/CILE is influenced by pH of the electrolyte within the range of 2.0 to 9.0 (Figure 5A). A pair of well-define redox peaks appeared, proving the realization of DET of Hb Fe(III)/Fe(II) electroactive center. The relationships of pH against peak current and potential are plotted in Figure 5B, which illustrates that Hb gave the highest redox peak currents at pH 2.0 and gradually decreased. Also, the linear relationship between $E^{0'}$ and pH was $E^{0'}$ (V) = -0.048 pH - 0.074 (n = 7, γ = 0.999). The slope value (-0.048 V pH^{-1}) is close to the theoretical result (-0.059 V pH^{-1}), demonstrating that the same protons and electrons are participated in the electrode reaction [27].

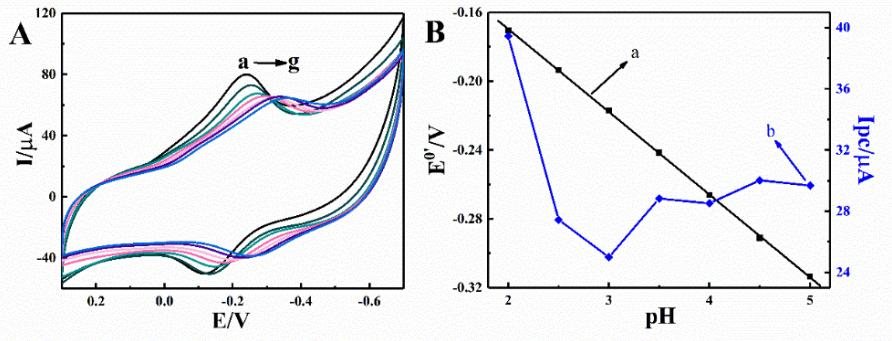

Figure 5. Cyclic voltammogram of (A) Nafion/Hb/FeS@MoS_2-C/CILE at different pH (a-g: 2.0, 2.5, 3.0, 3.5, 4.0, 4.5, 5.0); (B) (a) Linear relationship between $E^{0'}$ and pH, (b) Relationship between I*pc* and pH.

The effect of scan rate on CV responses of Nafion/Hb/FeS@MoS_2-C/CILE was investigated in PBS (pH 2.0) with curves present in Figure 6. The redox peak potentials moved towards positive and negative terminals with the increase of ΔEp value simultaneously, indicating that the electron transfer became more irreversible under faster scan rate. The redox peak currents increased proportionally with scan rate from 0.01 to 1.00 $V \cdot s^{-1}$, indicating a surface-controlled process [28]. Two linear regression equations were plotted as I_{pa} (μA) = -129.191 υ (V s^{-1}) - 3.844 (n = 11, γ = 0.992) and I_{pc} (μA) = 234.990 υ (V s^{-1}) + 11.366 (n = 11, γ = 0.991), respectively. The linear relationships of redox potential with lnυ were got as E_{pc} (V) = -0.055 lnυ (V s^{-1}) - 0.315 (n = 12, γ = 0.990) and E_{pa} (V) = 0.053 lnυ (V s^{-1}) - 0.001 (n = 12, γ = 0.992). Then electrochemical kinetic parameters were reckoned using Laviron's equations [29] with the results of the electron transfer number (n), the charge transfer coefficient (α) and the apparent heterogeneous electron transfer rate constant (*ks*) as 0.953, 0.493 and 1.89 s^{-1}. Therefore, the presence of FeS@MoS_2-C could result in favorable microenvironment for higher electron transfer rate of Hb with its specific structure and properties.

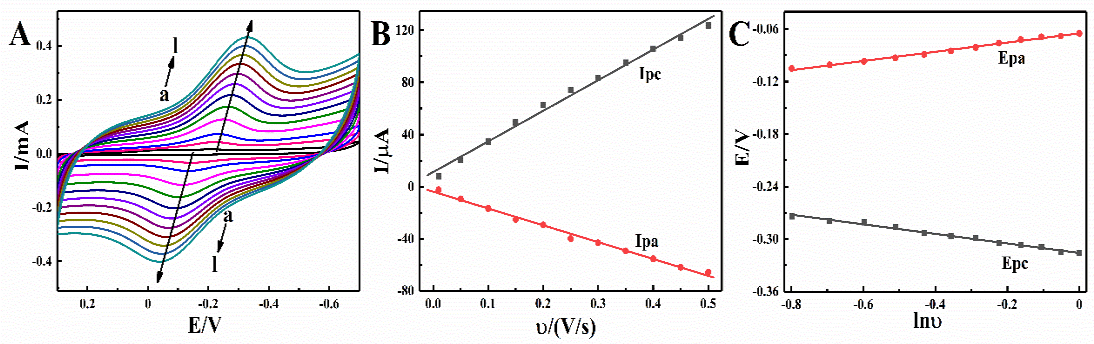

Figure 6. Cyclic voltammograms of Nafion/Hb/FeS@MoS_2-C/CILE (A) with different scan rate (a-l: 0.01, 0.05, 0.10, 0.20, 0.30, 0.40, 0.50, 0.60, 0.70, 0.80, 0.90, 1.00 V s^{-1}); the relationship (B) between Ip and υ, (C) between Ep and ln(υ).

3.5 Electrocatalysis

Electrocatalysis of Nafion/Hb/FeS@MoS_2-C/CILE to H_2O_2 was investigated with results present in Figure 7A. The continuous addition of H_2O_2 led to the decrease of oxidation peak and the increase of reduction peak. A good linear relationship of H_2O_2 concentration and the reduction peak currents was got in the range of 0.10 to 14.00 mmol·L^{-1} with the regression equation as I_{pc} (μA) = 4.298 C (mmol L^{-1}) + 19.550 (n = 15, γ = 0.993) and the detection limit as 0.033 mmol·L^{-1} (3σ). According to the Lineweaver-Burk equation, the Michaelis-Menten constant (K_M^{app}) value were got as 25.512 mmol·L^{-1}.

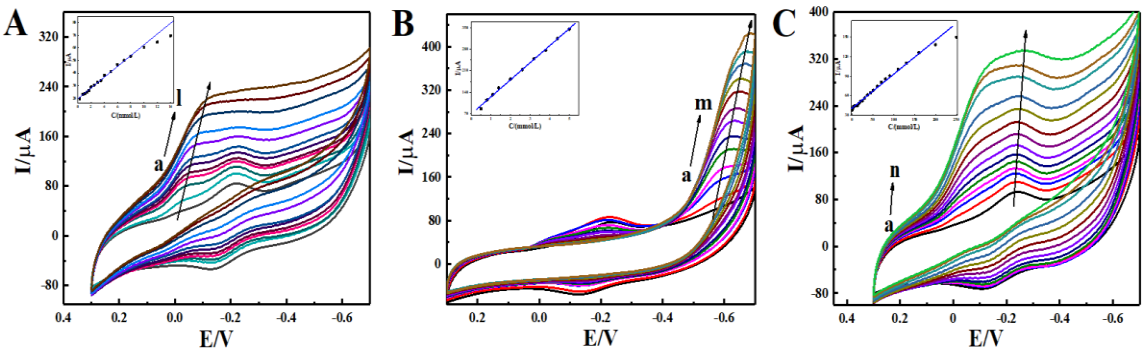

Figure 7. Cyclic voltammograms of Nafion/Hb/FeS@MoS_2-C/CILE with the addition of different concentrations of (A) H_2O_2 (a-l: 0, 0.10, 0.50, 1.10, 1.70, 2.50, 3.50, 5.00, 7.00, 10.00, 12.00, 14.00 mmol L^{-1}), inset is the linear relationship of reduction peak current versus H_2O_2 concentrations; (B) nitrite (a-m: 0, 0.10, 0.30, 0.50, 0.80, 1.10, 1.40, 2.00, 2.60, 3.20, 3.80, 4.40, 5.00 mmol L^{-1}), inset is the linear relationship of reduction peak current versus nitrite concentrations; (C) bromate (a-n: 0, 0.05, 0.35, 0.70, 1.30, 2.00, 3.00, 4.40, 6.00, 8.00, 11.00, 16.00, 20.00, 25.00 mmol L^{-1}), inset is the linear relationship of reduction peak current versus bromate concentrations

The modified electrode was used to catalyze different concentrations nitrite in pH 2.0 PBS. As shown in Figure 7B, CV current increased with nitrite concentration, and a good linear relationship was obtained between the reduction current and nitrite concentration ranging from 0.10 to 5.00 mmol L^{-1}

with a linear equation as I_{pc} (μA) = 55.83 C (mmol L^{-1}) + 68.77 (n = 10, γ = 0.997) and the detection limit as 0.057 mmol L^{-1}. The Michaelis-Menten constant (K_M^{app}) was calculated as 0.621 mmol L^{-1}. Table 1 lists the results of different modified electrodes for nitrite detection, indicating that the electrode has a relatively good analytical performance.

Table 1. Comparison of different modified electrodes for nitrite detection

Electrode	Linear range (mmol L^{-1})	Detection limit (mmol L^{-1})	Reference
Nafion/HRP/WS_2/CILE	1.50~4.00	0.20	[30]
CNF/Hemin/GCE	5.00~250	0.32	[31]
Nafion/HRP/Co_3O_4NP/CILE	0.10~1.10	0.20	[32]
RGO/GCE	8.90~167	1.00	[33]
CTS/Mb/SWCNHs/CILE	0.04~0.74	0.13	[34]
CTS/ELDH-GR-Hb/CILE	5.00-360	1.51	[35]
Nafion/Mb-HAp@CNF/CILE	0.30~10.00	0.23	[36]
Nafion/Hb/ FeS@MoS_2-C/CILE	0.10~5.00	0.057	This work

Hb-modified electrode also has good electrocatalytic ability to reduce bromate with its Hb Fe(III)/Fe(II) structure. The catalyze performance of Nafion/Hb/FeS@MoS_2-C/CILE to bromate was shown in Figure 7C. Good linear relationship to bromate concentration was got from 0.05 to 25.00 mmol L^{-1} with the regression equation as I_{pc} (μA) = 0.521 C (mmol L^{-1}) + 41.124 (n = 23, γ= 0.993) and the detection limit as 0.017 mmol L^{-1} (3σ). The K_M^{app} value were further got as 72.315 mmol L^{-1}.

3.6 Reproducibility and stability

The reproducibility was studied by five modified electrodes prepared independently with the relative standard deviation (RSD) as 4.76% for 0.1 mmol L^{-1} nitrite solution. The electrodes were tested after seven and fourteen days of storage in 4 ℃, and the currents decreased by 2.93% and 4.87%, respectively. The electrochemical response current decreased by 3.23% when one electrode was scanned for 40 times using cyclic voltammetry. The above results indicated that the modified electrodes exhibited good stability and reproducibility.

3.7 Actual samples

To verify the feasibility of Nafion/Hb/FeS@MoS_2-C/CILE in practical application, it was applied to detect nitrite concentrations in homemade pickle (bought at the market) with pickle juice as the sample. The analysis data are summarized in Table 2, in which the recovery of real samples was 95.33% to 100.01%, and the relative standard deviations (RSD) were less than 4.58%, showing the practical application of this modified electrode in real samples.

Table 2. Determination and recovery for nitrite of homemade pickle juice

Samples	Detected (mmol L^{-1})	Added (mmol L^{-1})	Total (mmol L^{-1})	Recovery (%)	RSD (%)
Pickle juice	0.050	0.100	0.143	95.33	2.17
		0.200	0.252	100.01	4.58
		0.300	0.346	98.86	3.12

4. CONCLUSIONS

In this paper, FeS@MoS_2-C composite was synthesized by one-step hydrothermal method, which was used for fabrication of electrochemical Hb sensor (Nafion/Hb/FeS@MoS_2-C/CILE). The petal structure of FeS@MoS_2-C has a large effective surface area and fast electron conductive ability with good biocompatibility. The catalytic effects of Nafion/Hb/FeS@MoS_2-C/CILE to various substrates including nitrite, H_2O_2, and bromate were investigated with detection limits of 0.057 mmol L^{-1}, 0.033 mmol L^{-1}, and 0.017 mmol L^{-1}, respectively. The excellent catalytic properties of the constructed electrodes can be used for pickle juice sample detection with good stability and reproducibility.

ACKNOWLEDGEMENTS
This work is supported by Hainan Provincial Natural Science Foundation (2019RC192), Scientific Research Projects of Higher Education Institutions in Hainan Province (Hnky2020ZD-12), Science and Technology project of Hainan Province (ZDYF2020217), the Open Foundation of Key Laboratory of Laser Technology and Optoelectronic Functional Materials of Hainan Province (2022LTOM01).

References

1. Y. Wang, H. Xu, J.M. Zhang, G. Li, *Sensors*, 8 (2008) 2043.
2. G. Hanrahan, D.G. Patil, J. Wang, *J. Environ. Monit.*, 6 (2004) 657.
3. M.D.T. Torres, W.R. de Araujo, L.F. de Lima, A.L. Ferreira, C. de La Fuente-Nunez, *Matter*, 4 (2021) 2403.
4. J. Monzó, I. Insua, F. Fernandez-Trillo, P. Rodriguez, *Analyst*, 140 (2015) 7116.
5. A. Arif, S. Salam, R. Mahmood, *Toxicol. In Vitro*, 65 (2020) 104810.
6. D.D. Haines, A. Tosaki, *Int. J. Mol. Sci.*, 21 (2020) 9698.
7. J.R. Winkler, H.B. Gray, *Chem. Rev.*, 114 (2014) 3369.
8. F. Shi, L.J. Yan, X.Q. Li, C.L. Feng, C.Z. Wang, B.X. Zhang, W. Sun, *J. Chin. Chem. Soc*., 68 (2021) 2006.
9. Y.C. Yao, C.X. Yin, S.G. Xu, M. Jiang, L. Zhu, R.Y. Zou, W. Sun, *Int. J. Electrochem. Sci.*, 17 (2022) 220546.
10. H. Xie, G.L. Luo, Y.Y. Niu, W.J. Weng, Y.X. Zhao, Z.Q. Ling, C.X. Ruan, G.J. Li, W. Sun, *Mater. Sci. Eng. C*, 107 (2020) 110209.
11. F. Shi, H. Cheng, Y.C. Yao, Z.J. Zhang, L.N. Zeng, L. Li, W. Sun, *Int. J. Electrochem. Sci.*, 17 (2022)220840.
12. Q.Y. Yu, R.Y. Zou, Y. He, H.J. Meng, B.X. Zhang, M.S. Ding, R.H. Zhou, W. Sun, *J. Hainan Norm. Univ., Nat. Sci.*, 34(2021)1
13. X.Q. Li, B. Shao, Y.X. Sun, B.X. Zhang, X.H. Wang, W. Sun, *Int. J. Electrochem. Sci.*, 16 (2021)210219.

14. H.A. Yones, L. Zhu, B. Shao, S.Y. Zhang, H. Xie, X.Q. Li, W. Sun, *Int. J. Electrochem. Sci.*, 16 (2021)210225.
15. L. Zhu, X.Y. Li, Y. Deng, R.Y. Zou, B. Shao, L.J. Yan, C.X. Ruan, W. Sun, *J. Iran. Chem. Soc*., 18 (2021) 1027.
16. L.P. Feng, L.X. Zhang, S. Chu, S. Zhang, X. Chen, Z.L. Du, Y.S. Gong, H. Wang, *Appl. Surf. Sci.*, 583 (2022) 152496.
17. H.S. Yang, J. Zhou, J. Bao, Y. Ma, J. Zhou, C.H. Shen, H.B. Luo, M. Yang, C.J. Hou, D.Q. Huo, *Microchem. J.*, 162 (2021) 105746.
18. X.N. Liu, L.J. Huang, Y.P. Wang, J. Sun, T.L. Yue, W.T. Zhang, J.L. Wang, *Sens. Actuators B,* 306 (2020) 127565.
19. H.L. Xiao, L.L. Cao, H.S. Qin, S.S. Wei, M. Gu, F.J. Zhao, Z.C. Chen, *J. Electroanal. Chem.*, 903 (2021) 115806.
20. Y.X. Guo, Z.Y. Yao, J. J. Brian, X. Sheng, L.Z. Fan, Y.Y. Li, F.G. Zhang, L.C. Sun, *Nano Energy*, 62 (2019) 282.
21. W.C. Wang, X.Q. Li, X.H. Yu, L.J. Yan, Z.F. Shi, X.Y. Wen, W. Sun, *J. Chin. Chem. Soc.*, 63 (2016) 298.
22. X.L. Guo, W.Y. Wang, K. Wu, Y.P. Huang, Q.Q. Shi, Y.Q. Yang, *Biomass Bioenergy*, 125(2019)34.
23. W.F. Dong, G. Chen, X. Hu, X.D. Zhang, W.B. Shi, Z.F. Fu, *Sens. Actuators B,* 305(2020)127530
24. L.D. Kong, Z.Y. Du, Z.Y. Xie, R.J. Chen, S.H. Jia, R.X. Dong, Z.L. Sun, W. Sun, *Int. J. Electrochem. Sci.*, 12 (2017) 2297
25. P.L. San Biagio, E. Vitrano, A. Cupane, F. Madonia, M.U. Palma, *Biochem. Biophys. Res. Commun.*, 77 (1977) 1158.
26. K. B. Oldham, *J. Electroanal. Chem.,* 105 (1979) 373.
27. R.A. Kamin, G.S. Wilson, *Anal. Chem.*, 52 (1980)1198.
28. X.J. Liu, T. Chen, L.F. Liu, G.X. Li, *Sens. Actuators, B,* 113(2006)106.
29. R.S. Nicholson, I. Shain, *Anal. Chem.*, 36 (1964) 706.
30. Y.Y. Niu, R.Y. Zou, H. A. Yones, X.B. Li, X.Y. Li, X.N. Niu, Y. Chen, P. Li, W. Sun, *J. Chin. Chem. Soc.*, 65 (2018) 1127
31. F. Valentini, L. Cristofanelli, M. Carbone, G. Palleschi, *Electrochim. Acta*, 63 (2012) 37.
32. W. Chen, W.J. Weng, C.X. Yin, X.L. Niu, G.J. Li, H. Xie, J. Liu, W. Sun, *Int. J. Electrochem. Sci.*, 13 (2018) 4741.
33. V. Mani, A. P. Periasamy and S.M. Chen, *Electrochem. Commun.*, 17 (2012) 75.
34. Y.Y. Li, X.S Liu, X.Y. Liu, N.N. Mai, Y.D. Li, W.Z. Wei, Q.Y. Cai, *Colloids Surf. B*, 88(2011)402.
35. T.R. Zhan, X.J. Wang, X.J. Li, Y. Song, W. Hou, *Sens. Actuators B*, 228(2016)101.
36. J. Liu, W.J. Weng, H. Xie, G.L. Luo, G.J. Li, W. Sun, C.X. Ruan, X.H. Wang, *ACS Omega*, 4(2019)15653.